Int. J. Electrochem. Sci., 13 **(2018)** 7246 – 7254, doi: 10.20964/2018.03.78

International Journal of
ELECTROCHEMICAL
SCIENCE
www.electrochemsci.org

Paper-based Microfluidic Immunoassay for Electrochemical Detection of B-type Natriuretic Peptide

Yong Zheng[1], *Zhen Huang* [1] *and Jidong Zhang*[2,*]

[1] Department of Cardiovascular Surgery, Affiliated Hospital of Taishan Medical University, Taian, Shandong, 271000, P.R. China
[2] Department of Cardiology, Affiliated Hospital of Qingdao University, Qingdao, Shandong, 266003, P.R. China
[*]E-mail: jidongzhangwuli@sina.com

Received: 4 October 2017 / *Accepted:* 12 November 2017 / *Published:* 5 June 2018

Heart failure has been acknowledged as a common disorder that leads to great morbidity and mortality. In heart failure and other cardiovascular disorders, effective biomarkers include cardiac natriuretic peptides, among which the most prominent one is B-type natriuretic peptide (BNP). The present study proposed the fabrication of a screen-printed working electrode (SPWE), with which a label-free and highly sensitive paper-based electrochemical immunosensor was successfully prepared. In addition, the SPWE was modified by amino functional graphene (NH_2-G)/thionine (Thi)/gold nanoparticles (AuNPs) nanocomposites, which led to the immobilization of anti-BNP and an enhancement in the determination sensitivity. The linear range and limit of detection (LOD) were determined to be 0.05 to 30 ng/mL and 0.012 ng/mL, with a corresponding correlation coefficient of 0.996.

Keywords: B-type natriuretic peptide; Microfluidic system; Electrochemical detection; Immunoassay; Congestive heart failure

1. INTRODUCTION

A series of clinical and fundamental studies have been carried out to study the pathophysiological and physiological functions of natriuretic peptides in clinical analysis and heart failure upon their identification. In spite of the substantial knowledge on B-type natriuretic peptide (BNP), no consensus has been reached on its utility [1-3]. The natriuretic peptide family is composed of D-type natriuretic peptide, C-type natriuretic peptide (CNP), BNP, and atrial natriuretic peptide (ANP). CNP is mainly synthesized in vessels, BNP and ANP are synthesized in the heart, and D-type

natriuretic peptide is isolated in atrial myocardium and plasma [4-6]. A separate gene encodes the precursor prohormone of each natriuretic peptide. As a 108 amino acid pro-hormone, BNP is separated into a 32 amino acid carboxy-terminal biologically active portion (BNP) and a 76 amino acid amino terminal part without biological activity, after being cleaved by the proteolytic enzyme furin [7, 8].

For normal clinical analysis, four commercially available assays for BNP have been reported to date. An enzyme immunoassay [9-11], a chemiluminescent immunoassay, or a rapid fluorescence immunoassay can be used for the detection of BNP, whereas an electrochemiluminescent assay is used for the detection of NT-proBNP [12, 13]. BNP and ANP play significant roles via their interaction with specific high-affinity receptors on target cells. At target sites and kidneys, three effective receptors have been recognized [14-17]. Located on cell membranes, the receptors include natriuretic receptor type A, natriuretic receptor type B, and type C—a clearance receptor—although they do not reflect their affinity for varying peptides [18-20]. The formation of cyclic guanylmonophosphate, leading to a majority of cardiovascular and renal effects of BNP and ANP, also suggests cellular physiological responses to natriuretic peptide stimulation [21, 22]. Natriuretic peptides are cleared from plasma by binding to natriuretic peptide receptors and through proteolysis by peptidases. The half-life of NT-proBNP is longer than that of BNP. At present, renal excretion is considered to be the major clearance mechanism of NT-proBNP. A shift in the relative BNP and NT-proBNP concentrations is found between heart failure patients and healthy individuals. In spite of the poorly understood shift significance, variations in the production of BNP and changes in its half-life and degradation resulting from receptor regulation might be the etiology of this observation.

Due to their high simplicity and specificity [23, 24], electrochemical immunosensors have gained substantial attention in the molecular recognition community as a promising substitute. A short detection time, low cost, and small size are other merits of these biosensors. In addition, no novel laboratory is needed for detection using electrochemical immunosensors, which could also facilitate point of care testing (POCT) [25, 26]. Nevertheless, based on previous reports, extensive application of electrochemical immunosensors in clinical detection has been rarely presented [27-30], possibly due to the requirement of simple albeit professional-level modifications, which are also required for immunosensor regeneration.

In the present study, a graphene-nanocomposite-coated screen-printed carbon working electrode (SPWE) was used to fabricate a highly sensitive, label-free electrochemical immunosensor based on a microfluidic paper analytical apparatus, which was then used for the determination of BNP. The SPWE was modified by NH_2-G/thionine (Thi)/AuNPs nanocomposites for the immobilization of anti-BNP, contributing to the high sensitivity of the sensor. For the determination mechanism of the developed immunosensor, the response current of Thi decreased in proportion to the concentrations of corresponding antigens because of the generation of an antibody–antigen immunocomplex. Therefore, the new immunosensor provides a promising approach toward point-of-care, specific, sensitive, and low-cost diagnostics for public health.

2. EXPERIMENTAL

2.1. Chemicals and instruments

A modified Hummers method was employed for the preparation of graphene oxide (GO), and the source material was graphite powder. Phosphate-buffered saline (PBS; 0.1 M Na_2HPO_4-NaH_2PO_4-KCl; pH 7.4) was synthesized from a PBS tablet. Bovine serum albumin (BSA), chitosan (CS), and thionine acetate (Thi) were obtained from Sinopharm Chemical Reagent Co., Ltd. (China). Commercial microfluidic paper was available in Li's lab. All other reagents were of analytical grade, and used without additional purification. A B-type natriuretic peptide ELISA kit was purchased from Tinashan Biotech Ltd. Co. and used according to the manufacturer's instructions. All measurements were conducted at room temperature. A CHI 660 electrochemical station (Autolab, Herisau, Switzerland) was used to perform cyclic voltammetry (CV) and differential pulse voltammetry (DPV) measurements.

2.2. Preparation of NH_2-G/Thi/AuNPs nanocomposites

Based on a previous report [31], a 15 nm AuNP solution was synthesized by the heat treatment of 250 mL of $HAuCl_4$ aqueous solution (1 mM), with 10 min of subsequent refluxing; 25 mL of trisodium citrate solution (40 mM) was rapidly added to the solution. After refluxing and stirring for another 15 min, the as-prepared solution was slowly cooled to ambient temperature. To remove excess water and ions, the solution was centrifuged. Several steps of centrifugation were followed by diluting the AuNPs using ethanol. Then, a 1.25% Nafion-AuNP solution was prepared by mixing 5% Nafion with the diluted AuNPs. A previously reported method was employed for the preparation of amino functional graphene [32]. Ethylene glycol (40 mL) was mixed with GO (one hundred milligrams) and ultrasonicated; ammonia water (1 mL) was then added to the mixture to obtain a dark-brown solution. Subsequently, this solution was placed into a Teflon-lined autoclave, and the reaction was maintained for 10 h at 180 °C. The precipitate produced after repeated filtering and washing was left to dry at 60 °C. NH_2-G/Thi nanocomposites were prepared by adding Thi solution (500 μL, 2 mg/mL) to a stable NH_2-G dispersion (500 μL, 1 mg/mL) under vigorous stirring for 1 d. Then, the non-integrated Thi molecules were removed. The as-prepared NH_2-G/Thi nanocomposites were subsequently dispersed in water (1 mL), to which the AuNP solution (5 mL) was added. The mixture was stirred for 12 h for the thorough combination of the amino groups of NH_2-G and AuNPs. This mixture was subsequently centrifuged and washed using high-purity water, with the obtained specimens re-dispersed in 500 μL CHIT solution (0.1%) and stored at 4 °C prior to future application.

2.3. Immunosensor fabrication and measurement

A carbon working electrode was modified with the stable NH_2-G/Thi/AuNPs (10 μL), followed by heating in an oven at 50 °C for 20 min (denoted NH_2/Thi/AuNPs-SPWE). Subsequently, anti-BNP (10 μL, 200 mg/mL) was dropped onto the corresponding area and stored at 4 °C in the refrigerator for

6 h. To obstruct potential remaining active sites and prevent non-specific adsorption, BSA (10 μL) was added at ambient temperature (denoted NH_2/Thi/AuNPs-SPWE-BSA-Ab). The sample without anti-BNP attached was denoted NH_2/Thi/AuNPs-SPWE-BSA. The obtained immunosensor was stored at 4 °C prior to use. Electrochemical measurements were carried out using a three-electrode configuration, in which the working and counter electrodes were screen-printed carbon electrodes and the reference electrode was a screen-printed Ag/AgCl electrode. Both CV and DPV measurements were carried out in PBS solutions (0.1 M, pH 7.4). The scan rate of the former measurement was 100 mV/s, whereas the parameters for the latter measurement were as follows: scan rate, 10 mV/s; interval time, 0.5 s; modulation time, 0.025 s; and modulation amplitude, 0.05 V. A quantitative analysis of BNP was performed using the peak currents of DPV. An automatic electrochemiluminescence instrument was used to detect the concentration of BNP in clinical serum specimens.

3. RESULTS AND DISCUSSION

Rapid and direct BNP detection was realized by a NH_2-G/Thi/AuNPs-modified SPWE after anti-BNP immobilization. Redox reactions involving Thi occurred on the electrode surface, generating an electric current. NH_2-G contributed to signal amplification through accelerated charge transfer, as it was highly biocompatible and conductive. Noncovalent attachment of Thi molecules onto the amino functional graphene surface occurred via π-π stacking interactions. In addition, interactions between Au and amino groups occurred, which resulted in the immobilization of AuNPs. The stability, activity, and immobilization results for different chemicals were obtained through CV measurement (performed in 2 mM $[Fe(CN)_6]^{4-}$/$[Fe(CN)_6]^{3-}$ (1:1) containing 0.1 M KCl) to study the electroactivity of the immunosensor, as shown in Fig. 1. The adsorption of protein led to a decrease in current response after blocking with BSA. Moreover, it proved the electroactive material was fixed tightly to the electrode surface and that the immunosensor could be used for further determination [33, 34].

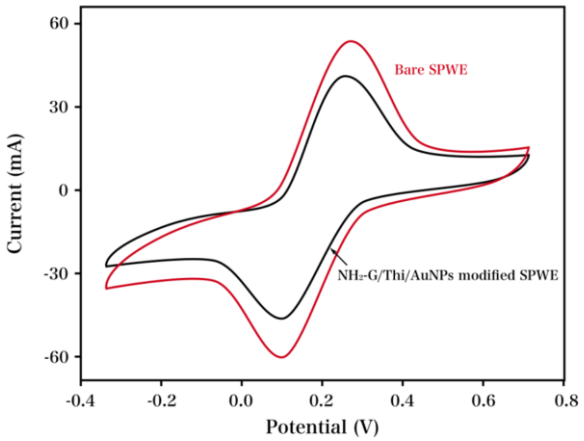

Figure 1. The electroactivities of the bare SPWE and NH_2-G/Thi/AuNP-coated SPWE based on CV in a hexacyanoferrate solution.

Fig. 2 shows the CVs of the coated SPWE in PBS (0.1 M, pH 7.4), which were used to investigate the electrode's electrochemical features. A well-defined reversible redox wave of Thi (oxidation peak potential, −0.16 mV; reduction peak potential, −0.26 mV) was observed for the NH_2-G/Thi/AuNP-coated SPWE, which was not recorded at the bare SPWE. In addition, the stable hybrid film showed a nano-porous structure, through which the current response could be enhanced after the electrode surface area was increased by the decrease in electrode impedance. According to the working principle of the electrochemical detection method we used, high concentrations of antigens could result in a low response.

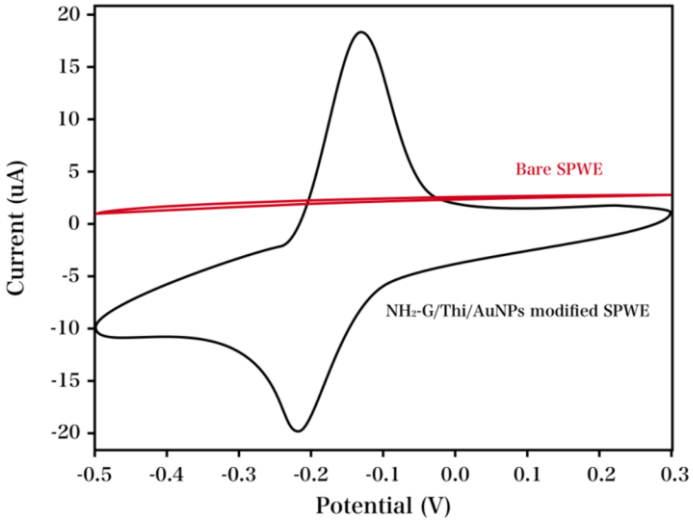

Figure 2. CV comparisons of the bare SPWE and NH_2-G/Thi/AuNPs-coated SPWE in 0.1 M of a pH 7.4 PBS solution. Scan rate: 50 mV/s.

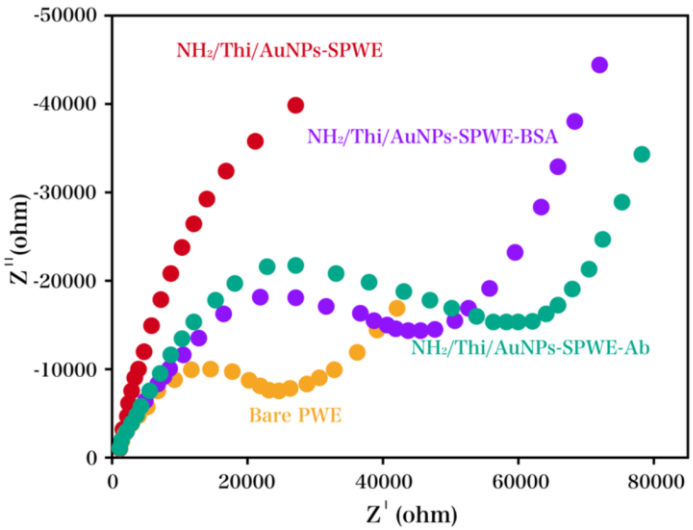

Figure 3. EIS profiles recorded for the bare SPWE, NH_2/Thi/AuNPs-SPWE, NH_2/Thi/AuNPs-SPWE-BSA, and NH_2/Thi/AuNPs-SPWE-Ab for the detection of 10 ng/mL BNP in pH 7.4 PBS containing 1 mM $K_3Fe(CN)_6$ (0.1 - 10^5 Hz).

Moreover, the current response could also be enhanced by the increased charge transfer due to the abundant NH_2-G. The oxidization and reduction peak currents were 17.5 and −17.2 μA, respectively. A comparable figure suggested that the redox reaction was perfectly reversible.

Fig. 3 shows the EIS profile for the preparation and assembly of the immunosensor, where the semicircular portion at high frequencies (the diameter suggests the electron transfer resistance) and linear portion at low frequencies correspond to the electrochemical processes subject to charge transfer and diffusion-limited electrochemical behavior. It is known that changes in electrochemical impedance reflect the chemical processes that occur in electrochemical sensors [35]. For comparison, each step of fabrication was studied, as the modification and assembly of the immunosensor were performed stepwise. Nearly linear Nyquist curves were obtained for the bare SPWE. On the other hand, the semicircle portions were reinforced after Ab and BSA were coated onto the electrode, which suggested that the electrode surface was successfully modified. Access to the electrode surface was decreased after Ab and BSA were coated, impeding charge transfer under this configuration. Electron transfer decreased with consecutive incubations with BSA, antigen and Ab. It is therefore clear that the assembly of these biomolecules on the surface of the electrode to form an immunosensor was successful [36].

The proposed immunosensor was used for BNP determination over a concentration range of 0.05 to 30 ng/mL, as shown in Fig. 4. As the concentration of BNP was increased, an increase in the amperometric signal was observed. For this sensor, the linear range was as wide as 0.05–30 ng/mL. Based on the signal-to-noise ratio, the LOD was determined to be 0.012 ng/mL, which suggested that the proposed sensor was highly sensitive and is more desirable than those reported in other studies [37, 38]. A linear calibration curve was recorded, and the correlation coefficient was determined to be 0.996. These results confirmed the desirable sensitivity of our proposed immunosensor toward the detection of BNP. For comparison with previous reports, the characteristics of different electrochemical sensors for AFP are summarized in Table 1.

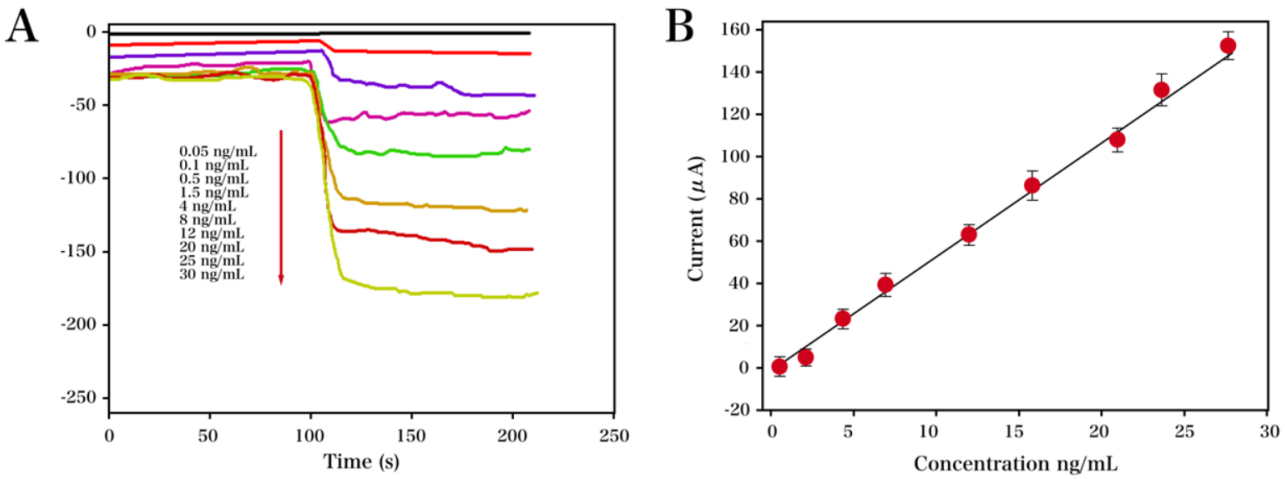

Figure 4. (A) Amperometric response recorded for our proposed sensor toward the detection of 0.05, 0.1, 0.5, 1.5, 4, 8, 12, 20, 25 and 30 ng/mL BNP in PBS containing 5 mM H_2O_2. (B) Calibration curve of the immunosensor.

Table 1. Comparison of the major characteristics of sensors used for the detection of BNP.

Electrode	Linear detection range	Detection limit	Reference
Magnetoimmunosensor	-	0.4761 ng/mL	[39]
ELISA	-	30.5 pg/mL	[40]
Streptavidin-modified SPCE	0 – 100 ng/mL	-	[41]
NH_2/Thi/AuNPs-SPWE-Ab	0.1 - 30 ng/mL	0.012 ng/mL	This work

The reproducibility of the sensor was studied by fabricating five electrodes under comparable conditions. After five measurements, the standard deviation was determined to be 4.8%, indicating desirable reproducibility. After storing the immunosensor in pH 7.4 PBS for 2 months at 4 °C, 92.5% of the initial value was retained, indicating desirable stability. These results confirmed that the proposed sensor has the potential of being used for future applications. A calibration curve was then plotted for the practical determination of four serum specimens. The determination was also carried out using a standard ELISA kit under comparable conditions. The performance of our proposed immunosensor was comparable to that of the standard ELISA kit (Table 2). This kit uses ELISA based on the biotin double antibody sandwich technology to assay human B-type natriuretic peptide. B-type natriuretic peptide is added to the wells, which are pre-coated with B-type natriuretic peptide monoclonal antibody, and then incubated. Anti B-type natriuretic peptide antibodies labeled with biotin are then added to link to streptavidin-HRP, which together form an immune complex. Unbound enzyme is removed after incubation and washed. The solution will then turn blue and then yellow due to the effects of the added acid. The shade of the solution and the concentration of human B-type natriuretic peptide are positively correlated. The relative error was determined to be below 5.1%, which further confirmed the practical suitability of our proposed immunosensor.

Table 2. Performance comparison of our proposed sensor and standard ELISA in the serum specimen determination (ng/mL)

Sample	1	2	3	4	5
The immunosensor	1.63	2.55	5.59	10.22	26.37
ELISA	1.71	2.62	4.65	10.24	26.11
Relative error (%)	4.7	2.3	5.1	2.3	4.1

4. CONCLUSIONS

In the present study, the electrochemical determination of BNP was realized using a state-of-the-art, label-free immunosensor based on a microfluidic paper analytical apparatus. The working

electrode was successfully modified by NH_2-G/Thi/AuNPs and was highly bioactive; thus, the sensor could be used for the determination of BNP. The correlation coefficient was determined to be 0.996 over a BNP concentration range of 0.05–30 ng/mL. Based on the signal-to-noise ratio, the LOD was determined to be 0.012 ng/mL.

References

1. A.Schimmel, M. Barents, M. de Jongste, J. Römer, R. Steward and F. Muskiet, *Clinical Chemistry*, 62 (2016) 407.
2. H. Røsjø, M. Dahl, M. Jørgensen, R. Røysland, J. Brynildsen, A. Cataliotti, G. Christensen, A. Høiseth, T. Hagve and T. Omland, *Clinical Chemistry*, 61 (2015) 1087.
3. A. Semenov and A. Katrukha, *Clinical Chemistry*, 62 (2016) 617.
4. A. Jaffe, F. Apple, A. Mebazaa and N. Vodovar, *Clinical Chemistry*, 61 (2015) 1016.
5. W. Taylor, D. Sutherland, H. Zhang and D. Hegedus, *Phytochemistry Letters*, 12 (2015) 105.
6. B. Winther and J. Reubsaet, *Journal of Separation Science*, 30 (2015) 234.
7. M. Filizola, N. Centeno and J. Perez, *Journal of Peptide Science*, 3 (2015) 85.
8. N. Kelleher, P. And and C. Walsh, *Journal of the American Chemical Society*, 120 (2016) 9716.
9. Tsai, ChingChung, Chang, LiChing, Huang, ShihChe, ShuLeei, Hsu and WenLi, *Molecules*, 20 (2015) 14504.
10. E. Aranarueda, A. Pedrote, L. Garcíariesco, Á. Arceleón, F. Guerreromárquez and J. Rodríguezrodríguez, *Medicina Clinica*, 145 (2015) 248.
11. S. den Boer, D. Rizopoulos, M. Du, A. Backx, A. Ten Harkel, G. van Iperen, L. Rammeloo, R. Tanke, E. Boersma and W. Helbing, *American Journal of Cardiology*, 118 (2016) 1723.
12. S. Susan, S. Khibar, D. Cathelijne, C. Valentina, M. Marco, M. Laura, D. Salvatore, J. Tijssen, Y. Pinto and W. Kok, *Journal of Cardiac Failure*, 21 (2015) 930.
13. M. Hezzell, A. Boswood, N. Lötter and J. Elliott, *Journal of Veterinary Cardiology*, 17 (2015) 34.
14. K. Reesukumal and B. Pratumvinit, *Clinical Laboratory*, 58 (2016) 1017.
15. Z. Bitar, O. Maadarani and K. Almerri, *Annals of Intensive Care*, 5 (2015) 1.
16. M. Dufang, W. Yongcheng, J. Ping, Y. Yonghui and L. Xiao, *International Heart Journal*, 57 (2016) 292.
17. M. D'Errico, M. Petruzzelli, E. Gianicolo, L. Grimaldi, F. Loliva, F. Tramacere, M. Andreassi, G. Pili, E. Picano and M. Portaluri, *International Journal of Radiation Biology*, 91 (2015) 804.
18. G. Lippi and F. Sanchis-Gomar, *International Journal of Cardiology*, 219 (2016) 111.
19. N. Nishii, M. Kubo, Y. Okamoto, S. Fujii, A. Watanabe, Y. Toyama, T. Yamada, M. Doi, H. Morita and H. Ito, *Circulation Journal*, 79 (2015) 1315.
20. C. Leufgen, U. Gembruch, B. Stoffelwagner, R. Fimmers and W.M. Merz, *Plos One*, 12 (2017) e0177253.
21. T. Meyer, C. Herrrmann-Lingen, M.L. Chavanon, K. Nolte, C. Pasedach, L. Binder, B. Pieske, G. Hasenfuss, R. Wachter and F. Edelmann, *Clinical Research in Cardiology*, 104 (2015) 1.
22. M. Smedsrud, J. Gravning, T. Omland, C. Eek, L. Mørkrid, H. Skulstad, L. Aaberge, B. Bendz, J. Kjekshus and T. Edvardsen, *International Journal of Cardiovascular Imaging*, 31 (2015) 967.
23. L. San, D. Zeng, S. Song, X. Zuo, H. Zhang, C. Wang, J. Wu and X. Mi, *Nanotechnology*, 27 (2016) 254003.
24. S. Tuteja, T. Duffield and S. Neethirajan, *Nanoscale*, 9 (2017)
25. W. Li, Y. Wang, F. Deng, L. Liu, H. Nan and H. Li, *Nano*, 10 (2015) 150710022232000.
26. N. Li, Y. Wang, W. Cao, Y. Zhang, T. Yan, B. Du and Q. Wei, *Journal of Materials Chemistry B*, 3 (2015) 2006.
27. W. Shen, Y. Zhuo, Y. Chai, Z. Yang, J. Han and R. Yuan, *Acs Applied Materials & Interfaces*, 7

(2015) 4127.
28. H. Huang, M. Liu, X. Wang, W. Zhang, D.P. Yang, L. Cui and X. Wang, *Nanoscale Research Letters*, 11 (2016) 507.
29. T. Feng, X. Qiao, H. Wang, Z. Sun, Y. Qi and C. Hong, *Journal of Materials Chemistry B*, 4 (2016) 990.
30. S. Zhou, Y. Wang and J. Zhu, *Acs Applied Materials & Interfaces*, 8 (2016) 7674.
31. L. Yang, X. Ren, F. Tang and L. Zhang, *Biosensors & Bioelectronics*, 25 (2009) 889.
32. X. Guo, Q. Wei, B. Du, Y. Zhang, X. Xin, L. Yan and H. Yu, *Applied Surface Science*, 284 (2013) 862.
33. J. Liu, J. Wang, T. Wang, D. Li, F. Xi, J. Wang and E. Wang, *Biosensors & Bioelectronics*, 65 (2015) 281.
34. L. Patricia and S. Ruth, *Bioelectrochemistry*, 101 (2015) 75.
35. M. Li, S. Biswas, M. Nantz, R. Higashi, X. Fu and A. Chem, *Analytical Chemistry*, 84 (2012) 1288.
36. Y. Liu, X. Weng, K. Wang, Y. Xue, A. Wang, L. Wu and J. Feng, *Sensors and Actuators B: Chemical*, 247 (2017) 349.
37. G. Zaid, A. Tanchilevitch, E. Rivlin, R. Gropper, U. Rosenschein, A. Lanir and E. Goldhammer, *International Journal of Cardiology*, 117 (2007) 157.
38. P. Mccullough, T. Omland and A. Maisel, *Reviews in Cardiovascular Medicine*, 4 (2003) 72.
39. E. Ávila, V. Escamilla-Gómez, V. Lanzone, S. Campuzano, M. Pedrero, D. Compagnone and J. Pingarrón, *Electroanalysis*, 26 (2014) 254.
40. T. Defrancesco, J. Rush, E. Rozanski, B. Hansen, B. Keene, D. Moore and C. Atkins, *Journal of Veterinary Internal Medicine*, 21 (2007) 243.
41. Y. Hartati, R. Nurmalasari, S. Gaffar and T. Subroto, *Procedia Technology*, 27 (2017) 149.